



Effect of Porous Medium Positioning on Heat Transfer of Micro-channel with Jet

M. Alibeigi, S. D. Farahani*

Department of Mechanical Engineering, Arak University of Technology, Arak, Iran

PAPER INFO

Paper history:

Received 26 May 2020

Received in revised form 16 June 2020

Accepted 03 August 2020

Keywords:

Micro-channel

Porous Media

Heat Transfer

Nano-Fluid

ABSTRACT

In this paper, the influence of the locating additive or placing porous-medium film on the heat transfer of a micro-channel by injecting fluid from its lower wall is investigated. The boundary condition slip-walls for the lower and higher walls of the micro-channel and orderly, as insulation and constant temperature is considered, respectively results show that the heat transfer increased with increasing Darcy number and the porous-medium film thickness. The consequences disclosed that the place of the porous-film has a substantial effect on heat transfer. The percentage changes observed for cases such the porous layer in the middle of the micro-channel, near the two upper and lower walls, near the upper wall, near the upper wall and in the form of a rib, along the length of the micro-channel with $L/3$ and $L/5$ is -14%, 2.25%, 5.46%, 55.53%, 70.5% and 86.27% for nusselt number compared to the porous layer-less state.

doi: 10.5829/ije.2020.33.10a.24

1. INTRODUCTION

In recent decades, with the development of electronic devices in very small dimensions, it is necessary to improve the conditions for the transfer of heat by using devices in the dimensions of the smallest increase. Microchannel heat exchangers can be used for this purpose. In addition, the use of new technologies such as nanotechnology has recently received a great deal of attention [1].

Numerous research sources have examined the effect of the cross-sectional shape of the channels, the location of the channels, the number of channels and the size and structure of the microchannel. Yang et al. [2] examined the performance of a microchannel heat transfer with needle-shaped blades in a laboratory and standard manner. Five different cross-sectional areas for needle-shaped blades were examined. They also used ionized water as a working fluid for cooling. Their results showed that the shape of the needle blades plays an important role in conveying heat transfer and fluid pressure drop. One of the results of their simulation, which is in good agreement with the laboratory results, is that the lowest

thermal resistance is related to geometries with hexagonal cross section and the lowest pressure point is related to circular geometry. Wang et al. [3] studied the effect of rectangular, trapezoidal and triangular geometries on the flow characteristics and heat transfer characteristics. After conducting experiments, they found that the microchannel with a rectangular cross-section had the lowest thermal resistance and best thermal performance. But it does increase the pressure drop. Chen et al. [4] simulated numerical and three-dimensional heat transfer and fluid flow within a microchannel with different cross sections. The results showed that the triangular microchannel had the best thermal performance and the rectangular section with the best performance. While the results of the work of Gonasgaren et al. [5], who also studied the effect of different geometries on the transfer properties of heat and current flow, showed that the microchannel performs the function with the cross section and the rectangular section had the highest transfer coefficient.

Many studies have been done to increase heat transfer from microchannels. One way is to use nanofluids, which can significantly increase heat transfer [6, 7]. Research

*Corresponding Author Institutional Email: sdfarahani@arakut.ac.ir
(S. D. Farahani)

on fluid flow and heat transfer in porous media has attracted the attention of many researchers in recent decades. Porous environment is a material consisting of a solid network connected by empty spaces or gaps between them. The empty spaces between the solid network allow fluid to flow into the network. In a natural porous environment, the distribution of pores is irregular in shape and size. Coastal sand, limestone and human lungs are examples of natural porous materials. Mathematical discovery in MCHS with the least square methods and numerical methods for chosen the best nano-fluid based on saturated porous medium was reported [8]. Usage of ZnO–water nano-fluids in corrugated channels with designing of the plate-fin heat exchangers with configuration of changing geometry such kinds of a) house-shaped channel, b) semicircular channel, c) trapezoidal channel, and d) straight channel were numerically studied [9].

The effects of solid phase generative heat on the generative entropy with an analytical model conferring to first law and second law of thermodynamics in micro-channel with porous water- Al_2O_3 nano-fluid flow in asymmetrically heated was developed. That exposed the minimization of generative entropy generative was the intensification of solid-phase generative heat supplementary reduces the discrepancy between the two models to less than 1% [10]. Represented nano-fluid through a horizontal porous micro-channel was studied for effects of magneto-fluid dynamics (MHD) arena and heat generation in the solid on the generated entropy by the heat transfer practices with an extensive variability of Re and Bejan number [11]. Mass transfer and forced heat transfer convection of Cu-water nano-fluid through a horizontal porous micro-channel considered which sound effects of numerous factors such as slip parameter, nanoparticle volume fraction, asymmetric heat flux and some dimensionless numbers such as Darcy number, Hartmann number, Brinkman number on total heat transfer and fluid flow profiles studied in details [12]. Shiriny et al. [13] examined the effect number of injection and number of volume fraction for maximum Nusselt number. Jalali et al. [14] observed that higher heat transfer coefficient was achieved by using 2.5 wt % Al_2O_3 nano-fluids compared to 1.0 wt % Al_2O_3 nano-fluids. There is also research on the production of hybrid nanoparticles and its effect on increasing heat transfer [15-18]. Shokouhmand et al. [19] investigated convective heat transfer and laminar flow by using lattice boltzmann method (LBM) in two channel configurations in a canal full of an inserting porous. Miroshnichenko et al. [20] studied effect of heat source and nanoparticle/water on free convection heat transfer within an inclined cavity. Nojoomizadeh et al. [21] examined the numerical forced convection heat transfer with Darcy number by blend of water and Fe_3O_4 nanoparticles in a two-dimensional micro-channel. Their conclusion was observing rise of

the slip velocity in the semi-upper and a decrease in the slip velocity in the semi-lower of the micro-channel [21]. The principal of liquid and solid phases on the heat transfer progression, investigators had assumed a two-phases model for the nano-fluid flow for assessment of temperature and velocity differences in two phases of the liquid and solid phases. In fact, the relative velocity and temperature of each phase was negligible [22-24]. A three-dimension porous-heat sink model identified the ideal geometric parameters of the micro-channel as a heat sink filled with porous medium by using a combination including an optimization approach of simplification of the conjugate-gradient method [25].

According to the previous literature, little research has been done on the position of the porous material on the heat transfer in the microchannels. In this study, the influence of using porous medium in three cases, which porous-medium the position of locating of porous such close to the upper and lower walls, placing porous medium middle of the micro-channel and placing porous medium selectively on dividable section on the amount of heat transfer is investigated. A two-dimensional micro-channel on the lower wall with several openings for fluid injection is considered. The lower wall of micro-channel resumed the insulation wall and the upper wall have a constant temperature and slip boundary condition on the walls is deliberated. The combination of nanoparticle with water is also considered as working fluids. The porous-film thickness on the heat transfer from the channel is examined. Numerical simulation is performed by using Comsol software where solution of its is finite element method (FEM).

2. MATERIALS AND METHODS.

In this study, a two-dimensional micro-channel with porous medium and injection with inlet velocity u_c and three different jet inlet velocities $u_d = 0.5u_c$ considered.

A schematic of the physical models of the problem under study is shown in Figure 1. For the micro-porous channel, three cases have been given. Firstly, the porous medium with two separated walls has two states: 1. near the upper and lower walls with two equal separated τ thickness layer (Figure 1(a)); 2. in the middle of the micro-channel with putting two side nearly in the middle with 2τ thickness (Figure 1(b)). Secondly, the porous medium with one wall has two states 1. near the upper wall with τ thickness (Figure 1(c)); 2. near the upper wall with τ thickness and adding a ribbed τ thickness with $N=100$ teeth to the one-sided porous (Figure 1(d)). Thirdly, the porous medium with two separated walls with distinguishing rather than the first case with $\tau = H$ thickness the has two states: 1. divided the channel by 3 equal sections and put the porous layer in the middle

section(Figure 1(e)); 2. divided the channel by 5 equal sections and the porous layer one in between puts in the periodically distance in two L/5 section (Figure 1(f)). The material is porous medium of aluminium foam. In Figure 1, orderly H_0 , τ , H , L and D are the thickness of non-porous media, the thickness of porous media, micro-channel width, micro-channel length and $D=0.007L$ is the diameter of each injection. From the lower wall of the micro-channel there are three openings for injections τ is chosen $\tau = H \times (0.05, 0.1, 0.2, 0.3, 0.4)$ in this case.

Momentum, continuity and energy equations that are major equations following as:

$$u \frac{\partial u}{\partial x} + v \frac{\partial u}{\partial y} = -\frac{\partial p}{\partial x} + \frac{1}{\text{Re}} \left(\frac{\partial^2 u}{\partial x^2} + \frac{\partial^2 v}{\partial y^2} \right) \quad (1)$$

$$\frac{\partial u}{\partial x} + \frac{\partial v}{\partial y} = 0 \quad (2)$$

$$u \frac{\partial T}{\partial x} + v \frac{\partial T}{\partial y} = -\frac{\partial p}{\partial x} + \frac{1}{\text{Re Pr}} \left(\frac{\partial^2 T}{\partial x^2} + \frac{\partial^2 T}{\partial y^2} \right) \quad (3)$$

The dimensionless parameters mostly used in this numerical study are:

$$X = \frac{x}{L}, Y = \frac{y}{H}, L^* = \frac{L}{H}, \beta^* = \frac{\beta}{H} \quad (4)$$

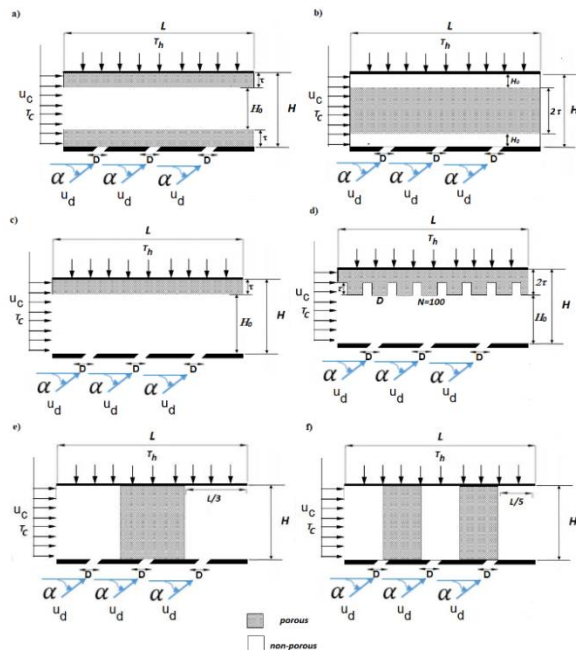


Figure 1. 2-D shemata of micro-channel with different position of porous layer

$$Y = \frac{y}{H}, H^* = \frac{H_0}{H}, \tau^* = \frac{\tau}{H} \quad (5)$$

$$U = \frac{u}{u_c}, V = \frac{v}{v_c}, U_d = \frac{u_d}{u_c}, V_d = \frac{v_d}{v_c}, P = \frac{\Delta p}{\rho_{nf} u_c^2} \quad (6)$$

$$\theta = \frac{T - T_c}{T_h - T_c}, \text{Re} = \frac{u_c H}{\nu_f}, \text{Pr} = \frac{\nu_f}{\alpha_f} \quad (7)$$

In heat transfer the most significant dimensionless number is local Nusselt number which defined as follows: [9]

$$Nu(x) = \frac{hD_h}{k} \quad (8)$$

where D_h and k are the hydraulic diameter, heat transfer convection coefficient and thermal conductivity. In this case, the dimensionless boundary conditions are:

$$U_c = 1, \quad V = 0, \quad \theta = 0 \quad \text{For } X=0, 0 \leq Y \leq 1 \quad (9)$$

$$\frac{\partial U}{\partial X} = 0, \quad V = 0, \quad \frac{\partial \theta}{\partial Y} = 0 \quad \text{For } X=L^*, 0 \leq Y \leq 1 \quad (10)$$

$$U_s = \beta^* \left(\frac{\partial U}{\partial Y} \right)_{Y=0}, \quad V = 0, \quad \frac{\partial \theta}{\partial Y} = 0 \quad \text{For } Y=0, 0 \leq X \leq L^* \quad (11)$$

$$U_s = \beta^* \left(\frac{\partial U}{\partial Y} \right)_{Y=1}, \quad V = 0, \quad \theta = 1 \quad \text{For } Y=1, 0 \leq X \leq L^* \quad (12)$$

the boundary conditions of the injection jets bounded by,

$$U_d = 0.5 \cos(\alpha), \quad V_d = 0.5 \cos(\alpha), \quad \theta = 0 \quad (13)$$

When the working fluid is the nanofluid, nanofluid properties are given in Table 1 in terms of nanofluid volume fraction, ϕ .

Representively, adding porous material to the micro-channel the dimensionless momentum equation is [26]:

TABLE 1. Thermophysical properties of nano-fluid ZnO/Water [9]

Volume fraction	$\phi = 0$	$\phi = 1\%$	$\phi = 3\%$	$\phi = 5\%$
Density ($\frac{kg}{m^3}$)	998.2	1043.1	1135.2	1037.6
Viscosity (Pa.s)	$8.9E^{-4}$	$9.1265E^{-4}$	$9.6042E^{-4}$	0.001
Specific Heat (J/kg.k)	4182	3981.2	3633.8	3338.5
Conductivity (w/m.k)	0.6	0.7360	0.9846	1.23

TABLE 2. Thermophysical properties of porous material [27, 28]

ρ_p (kg / m ³)	$c_{p,p}$ (J / kg.K)	k_p (W / m.k)	κ (m ²)	ε_p
400s	400	5.8	10 ⁻⁵	0.8

$$-\frac{\partial P}{\partial X} + \mu_{eff} \frac{\partial^2 U}{\partial Y^2} + \frac{\mu_f}{\kappa} U = 0 \tag{19}$$

The conservation energy is:

$$\nabla \cdot ((\rho c_p)_{eff} uT) = \nabla \cdot (k_{eff} \nabla T) \tag{20}$$

Where μ_{eff} is the dynamic viscosity of the porous medium, phase which has been chosen and κ is the permeability the equilibrium of heat transfer between the porous medium and the nanofluid, the thermal effectiveness conductivity k_{eff} can be determined using the following equation [26]:

$$k_{eff} = (1 - \varepsilon_p) k_p + \varepsilon_p k_{nf} \tag{21}$$

Where ε_p is the porosity of porous media part along the micro-channel and, the dimensionless Nusselt number for adding porous to the nanofluid defined as:

$$Nu = -\frac{k_{eff}}{k_f} \frac{\partial \theta}{\partial Y} \Big|_Y = Y_0 \tag{22}$$

Representively, the Brownian motion calculated the slip velocity U_s by following equation [29].

$$U_s = \frac{2k_b T}{\pi \mu_f d_s^2} \tag{23}$$

where the Boltzmann constant $k_b = 1.3807 \times 10^{-23}$ J/K and $d_s = 40$ nm, the Darcy number for this case defined as:

$$Da = \frac{\kappa}{D_h^2} \tag{24}$$

where D_h is the hydraulic diameter.

Finite element method with PARDISO algorithm used. Discretization P1+P1 method with maximum residual of 10⁻³ was used. Also, near the slip walls the mesh determined finer than the others additionally, the effect of changing nanoparticle with volume fraction various. Changing of base fluid in the end, adding of Aluminum porous foam on the nanoparticles for enhancing heat transfer were investigated, temperature, and streamlines contours and Nusselt number curves are presented.

3. GRID INDEPENDENCY

In numerical solution, the triangle meshes with boundary layer meshes near to the walls was chosen, the size of the mesh affects the accuracy and time of the solution. The smaller the mesh, the more accurate the solution becomes, but the time required to solve it also increases. To ensure accuracy, the grid study for averaged Nusselt number is presented in Table 3. A 50 × 500 grid has been used to continue the study.

4. RESULTS

In this study, the effect of porous medium layer on heat transfer from a two-dimensional micro-channel is explored. To make sure the accuracy of the numerical solution presented in this numerical study, the results of the present numerical solution were compared with shiriny et al. [13]. This comparison was made for the case where the Reynolds number is 100 and illustrated in Figure 2. At this point is a moral match between the results of the present study and the reference and there is less than 7% difference.

Figures 3. displays for the slip velocity and Nusselt number changes with the change of the nano-fluid volume fraction. Volume fractions of 1, 3, and 5 percent are taken. It can be realized that with increasing volume fraction, Nusselt number has been reduced 2.017% cause of the increasing k in the equation (24). The slip velocity has any changing with alternative of volume fraction. Volume fraction changes do not have a substantial effect on slip velocity. Figures 4 shows changes in slip velocity and Nusselt number by τ^* nearby the micro-channel walls. The working fluid is water. As τ^* increases, the gradient of temperature changes on the surface increases, which leads to an increase in heat transfer coefficient. The gradient of the velocity modifications on the surface decreases, which directs to a reduction in the slip velocity. It can be observed increasing the thickness of the porous medium layer, the Nusselt number increased for each τ^* about 13.4% and the slip velocity for each τ^* decreased 9.99%. The transfer coefficient of heat transfer is higher in systems be made of porous media. One of the vital reasons for this is the increase in the porous media for thermal conductivity factor.

TABLE 3. The nusselt average for different position of porous H for $\varphi = 5\%$, $Re = 100$, $\beta^* = 0.1$

Grid	10×100	50×500	75×1000
Middle	5.2566	5.2351	5.236
Two-sided	4.9642	4.9492	4.948

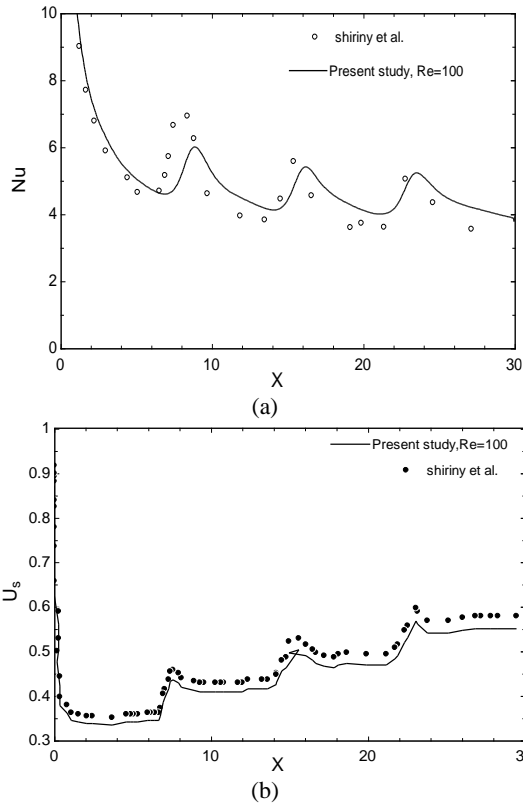


Figure 2. Validation of numerical solution results a)Nu and b)slip velocity for Re=100

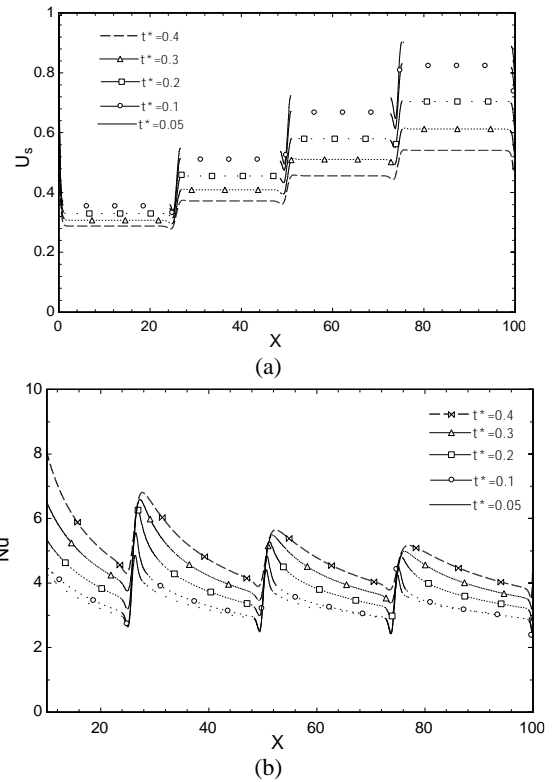


Figure 4. Variations of Nusselt number and slip velocity with porous layer thickness for two-sided porous

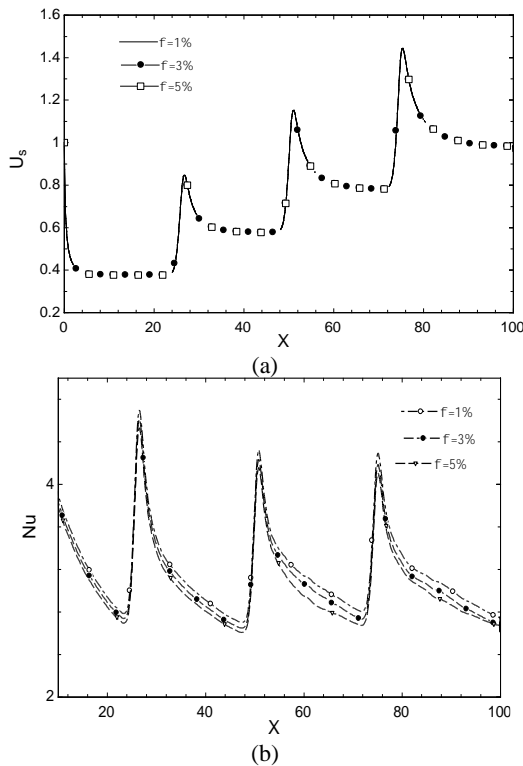


Figure 3. Variations of Nusselt number and slip velocity with nano fluid volume fraction

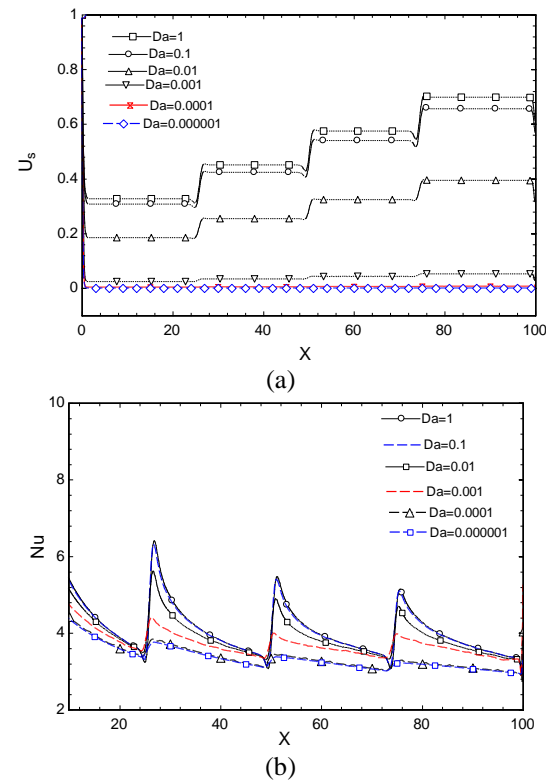


Figure 5. Variations of Nusselt number and slip velocity with Darcy number for two-sided porous with $\tau^* = 0.2$

Figure 5. indicates the effect of permeability on the Nusslet number and slip velocity. The Darcy number has been utilized to variation of the permeability. With cumulative Da number as shown, the fluid flows more simply and the boundary layer becomes thinner. By accumulative the permeability of the porous solid-wall temperature furthermore, the overall heat transfer increases from the mini-channel. An increase in Darcy's number leads to an increase in U_s and Nu . Figure 6 shows that the changes in heat transfer coefficient and slip velocity are similar for both porous layer placement states; close to the horizontal wall and the central wall of the micro-channel.

As the porous-film thickness of the porous medium on the rise, the slip velocity reduces and the heat transfer coefficient increases. As revealed in Figure 1., for more comparison divided the channel two cases, divided by 3 equal sections and putting the porous medium in the middle section and divided the channel by 5 equal sections and putting two porous medium in the section 2, 4. It has been compared two case with non-porous medium and shown the nusslet number and slip velocity in figure and made known as the enhancing supremely the Nusslet number against the non-porous micro-channel cause of the interface of fluid with the impact of porous medium intensification of heat transfer shown in Figure 7. The average nusslet number for three sections

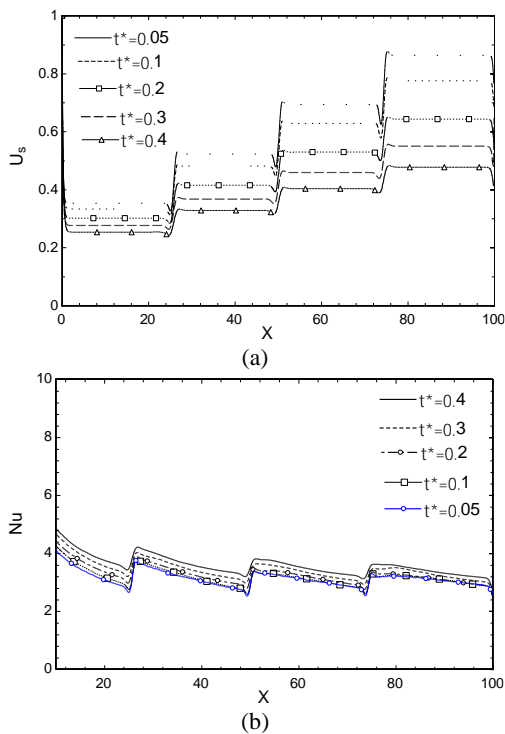


Figure 6. Variations of Nusselt number and slip velocity with thickness of porous layer for middle porous

is about 7.1784 and for five sections is 7.8422 against the non-porous has been 4.2138 shown that increasing 70.35% Nusselt number for three sections and increasing 86.10% versus non-porous. For slip velocity increased for more impact of fluid and porous media shown in Figure 7. In addition, almost in $X=80$ the flow has been fully developed and the slip velocity shall be constant till the end of micro-channel.

Slip velocity variations and Nusselt number have been studied for the case where the porous medium layer is just near the top wall and is ribbed, and the results were compared in Figure 8. When the porous layer is close to the wall, amount of the heat transfer factor is greater than when the porous-film layer is in the medium of the channel. The presence of a rib causes a pattern of flow change and turbulence in the flow, which direct to a change in the field of velocity and temperature. The percentage change in the number of nussult is observed for cases where the porous layer in the central of the micro-channel, near the two longitudinal-walls and inferior-walls, near the upper wall, and near the upper wall and in the form of a rib is -14%, 2.25%, 5.46% and 55.53%, respectively, compared to the porous layer-less state. The highest heat transfers and slip velocity in Figure 7. are associated to the instance of the porous layer is in the form of a rib.

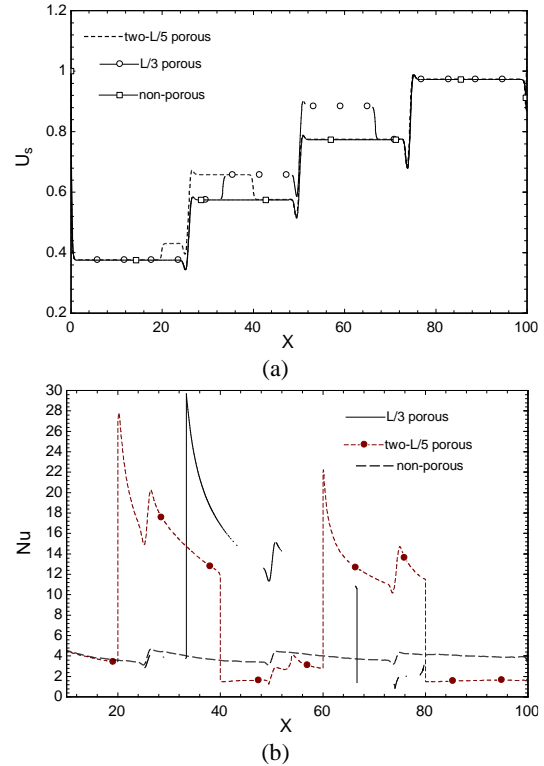


Figure 7. Variations of Nusselt number and slip velocity with porous medium intensification of heat transfer

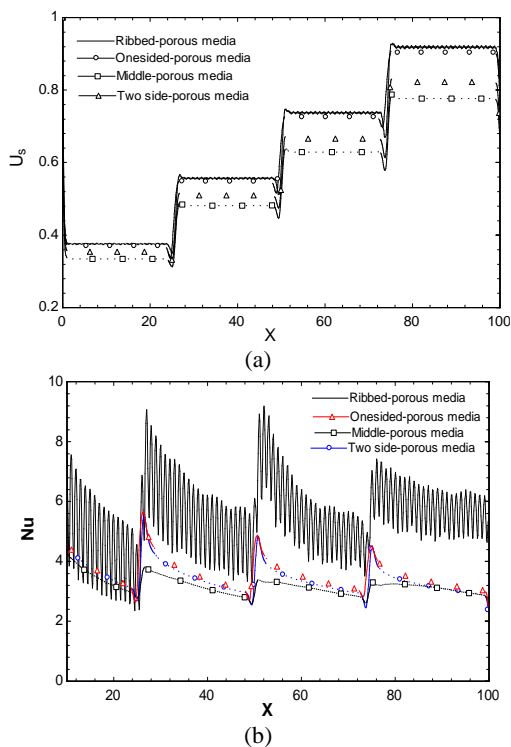


Figure 8. Variations of Nusselt number and slip velocity with the changing placing of porous layer thickness

5. CONCLUSIONS

In this study, the efficacy of the position of the porous material within a microchannel on heat transfer characteristics was analyzed. A number of several placing of the porous layer were tested. Modeling has been operated in the Comsol software with finite element method. The demonstration results with enlarging the amount of ϕ , dimensionless Nu number decreased. As the porous-film medium thickness rises, the heat transfer factor grows and the slip velocity decreases. Changes in heat transfer and slip velocity are proportional to the change in Da . Heat transfer is greater by placing a porous layer near the wall than in the center of the channel. The highest heat transfer is in the case where the porous layer is located along the length of the micro-channel with $L/5$ and heat transfer enhancement is 86.27%. It is specified that the amount of heat transfer from the micro-channel is a strong function of how the porous medium is located. Eventually, in near future of micro-channel with porous-medium the position of locating of porous cause of enhancement heat transfer will be important. It will be settled instead of the heat sinks, steam methane reforming reactor, nanoelectromechanical systems (NEMS)-based, microelectromechanical systems (MEMS), MHD properties and heat exchangers such as plate-pin heat exchanger.

6. REFERENCES

- Tuckerman, D.B. and Pease, R.F.W., "High-performance heat sinking for vlsi", *IEEE Electron Device Letters*, Vol. 2, No. 5, (1981), 126-129. <http://dx.doi.org/10.1108/HFF-04-2018-0149>
- Yang, D., Wang, Y., Ding, G., Jin, Z., Zhao, J. and Wang, G., "Numerical and experimental analysis of cooling performance of single-phase array microchannel heat sinks with different pin-fin configurations", *Applied Thermal Engineering*, Vol. 112, (2017), 1547-1556. <http://dx.doi.org/10.1016/j.applthermaleng.2016.08.211>
- Wang, H., Chen, Z. and Gao, J., "Influence of geometric parameters on flow and heat transfer performance of micro-channel heat sinks", *Applied Thermal Engineering*, Vol. 107, (2016), 870-879. <https://doi.org/10.1016/j.applthermaleng.2016.07.039>
- Chen, Y., Zhang, C., Shi, M. and Wu, J., "Three-dimensional numerical simulation of heat and fluid flow in noncircular microchannel heat sinks", *International Communications in Heat and Mass Transfer*, Vol. 36, No. 9, (2009), 917-920. <https://doi.org/10.1016/j.icheatmasstransfer.2009.06.004>
- Gunnasegaran, P., Mohammed, H., Shuaib, N. and Saidur, R., "The effect of geometrical parameters on heat transfer characteristics of microchannels heat sink with different shapes", *International Communications in Heat and Mass Transfer*, Vol. 37, No. 8, (2010), 1078-1086. <http://dx.doi.org/10.1016%2Fj.icheatmasstransfer.2010.06.014>
- Masuda, H., Ebata, A., Teramae, K., Hishinuma, N. and Ebata, Y., "Alteration of thermal conductivity and viscosity of liquid by dispersing ultra-fine particles (dispersion of γ - Al_2O_3 , SiO_2 and TiO_2 ultra-fine particles)", *Netsu Bussei* 1993 Vol. 7, No. 4, (1993). <https://doi.org/10.2963/jjtp.7.227>
- Khanafar, K., Vafai, K. and Lightstone, M., "Buoyancy-driven heat transfer enhancement in a two-dimensional enclosure utilizing nanofluids", *International Journal of Heat and Mass Transfer*, Vol. 46, No. 19, (2003), 3639-3653. [https://doi.org/10.1016/S0017-9310\(03\)00156-X](https://doi.org/10.1016/S0017-9310(03)00156-X)
- Pourmehran, O., Rahimi-Gorji, M., Hatami, M., Sahebi, S. and Domairry, G., "Numerical optimization of microchannel heat sink (mchs) performance cooled by kkl based nanofluids in saturated porous medium", *Journal of the Taiwan Institute of Chemical Engineers*, Vol. 55, (2015), 49-68. <https://doi.org/10.1016/j.jtice.2015.04.016>
- Ajeel, R.K., Salim, W.-I. and Hasnan, K., "Comparative study of the thermal performance of corrugated channels using ZnO-water nanofluid", *Journal of Thermophysics and Heat Transfer*, Vol. 33, No. 2, (2019), 508-516. <https://doi.org/10.2514/1.T5497>
- Ting, T.W., Hung, Y.M. and Guo, N., "Entropy generation of viscous dissipative nanofluid convection in asymmetrically heated porous microchannels with solid-phase heat generation", *Energy Conversion and Management*, Vol. 105, (2015), 731-745. <https://doi.org/10.1016/j.enconman.2015.08.022>
- Hosseini, S., Ghasemian, M., Sheikholeslami, M., Shafee, A. and Li, Z., "Entropy analysis of nanofluid convection in a heated porous microchannel under mhd field considering solid heat generation", *Powder Technology*, Vol. 344, (2019), 914-925. <https://dx.doi.org/10.1016/j.powtec.2018.12.078>
- Moshizi, S., "Forced convection heat and mass transfer of mhd nanofluid flow inside a porous microchannel with chemical reaction on the walls", *Engineering Computations*, (2015). <https://doi.org/10.1108/02644401211246283>
- Shiriny, A., Bayareh, M. and Nadooshan, A.A., "Nanofluid flow in a microchannel with inclined cross-flow injection", *SN Applied Sciences*, Vol. 1, No. 9, (2019), 1015. <https://doi.org/10.1007/s42452-019-1050-y>

14. Jalali, E. and Karimipour, A., "Simulation the effects of cross-flow injection on the slip velocity and temperature domain of a nanofluid flow inside a microchannel", *International Journal of Numerical Methods for Heat & Fluid Flow*, (2019). <http://dx.doi.org/10.1108/HFF-04-2018-0149>
15. Barzegar, M.H. and Fallahiyekta, M., "Increasing the thermal efficiency of double tube heat exchangers by using nano hybrid", *Emerging Science Journal*, Vol. 2, No. 1, (2018), 11-19. <https://doi.org/10.28991/esj-2018-01122>
16. Manikandan, G., Yuvashree, M., Sangeetha, A., Bhuvana, K. and Nayak, S.K., "Liver tissue regeneration using nano silver impregnated sodium alginate/pva composite nanofibres", *SciMedicine Journal*, Vol. 2, No. 1, (2020), 16-21. <https://doi.org/10.28991/SciMedJ-2020-0201-3>
17. Kostikov, Y.A. and Romanenkov, A.M., "The technology of calculating the optimal modes of the disk heating (ball)", *Civil Engineering Journal*, Vol. 5, No. 6, (2019), 1395-1406. <https://doi.org/10.28991/cej-2019-03091340>
18. Su, C. and Cheng, Y.-h., "Numerical and experimental research on convergence angle of wet sprayer nozzle", *Civil Engineering Journal*, Vol. 4, No. 9, (2018), 1985-1995. <https://doi.org/10.28991/cej-03091132>
19. Shokouhmand, H., Jam, F. and Salimpour, M., "The effect of porous insert position on the enhanced heat transfer in partially filled channels", *International Communications in Heat and Mass Transfer*, Vol. 38, No. 8, (2011), 1162-1167. <http://dx.doi.org/10.1016/j.icheatmasstransfer.2011.04.027>
20. Miroshnichenko, I.V., Sheremet, M.A., Oztop, H.F. and Abu-Hamdeh, N., "Natural convection of Al₂O₃/H₂O nanofluid in an open inclined cavity with a heat-generating element", *International Journal of Heat and Mass Transfer*, Vol. 126, No., (2018), 184-191. <https://doi.org/10.1016/j.ijheatmasstransfer.2018.05.146>
21. Nojoomizadeh, M., Karimipour, A., Firouzi, M. and Afrand, M., "Investigation of permeability and porosity effects on the slip velocity and convection heat transfer rate of fe3o4/water nanofluid flow in a microchannel while its lower half filled by a porous medium", *International Journal of Heat and Mass Transfer*, Vol. 119, (2018), 891-906. <https://doi.org/10.1016/j.ijheatmasstransfer.2017.11.125>
22. Kalteh, M., Abbassi, A., Saffar-Avval, M. and Harting, J., "Eulerian-eulerian two-phase numerical simulation of nanofluid laminar forced convection in a microchannel", *International Journal of Heat and Fluid Flow*, Vol. 32, No. 1, (2011), 107-116. <https://doi.org/10.1016/j.ijheatfluidflow.2010.08.001>
23. Moshizi, S., Malvandi, A., Ganji, D. and Pop, I., "A two-phase theoretical study of al₂o₃-water nanofluid flow inside a concentric pipe with heat generation/absorption", *International journal of thermal sciences*, Vol. 84, (2014), 347-357. <https://doi.org/10.1016/j.ijthermalsci.2014.06.012>
24. Rashidi, M., Hosseini, A., Pop, I., Kumar, S. and Freidoonimehr, N., "Comparative numerical study of single and two-phase models of nanofluid heat transfer in wavy channel", *Applied Mathematics and Mechanics*, Vol. 35, No. 7, (2014), 831-848. <https://doi.org/10.1007/s10483-014-1839-9>
25. Hung, T.-C., Huang, Y.-X., Sheu, T.-S. and Yan, W.-M., "Numerical optimization of the thermal performance of a porous-microchannel heat sink", *Numerical Heat Transfer, Part A: Applications*, Vol. 65, No. 5, (2014), 419-434. <https://doi.org/10.1080/10407782.2013.836005>
26. Guo, Z., Saunders, N., Miodownik, A. and Schillé, J., *Aluminium alloys, their physical and mechanical properties*, j. Hirsch, b. Skrotzki, and g. Gottstein, ed. 2008, Wiley-VCH.
27. Mohammed, R.H., Mesalhy, O., Elsayed, M.L., Huo, R., Su, M. and Chow, L.C., "Performance of desiccant heat exchangers with aluminum foam coated or packed with silica gel", *Applied Thermal Engineering*, Vol. 166, (2020), 114626. <https://doi.org/10.1016/j.applthermaleng.2019.114626>
28. Nield, D.A. and Bejan, A., "Convection in porous media", Springer, Vol. 3, (2006). <https://doi.org/10.1007/978-1-4614-5541-7>
29. Brinkman, H., "The viscosity of concentrated suspensions and solutions", *The Journal of Chemical Physics*, Vol. 20, No. 4, (1952), 571-571. <https://doi.org/10.1063/1.1700493>

Persian Abstract

چکیده

در این مقاله اثر لایه متخلخل بر روی انتقال حرارت یک میکروکانال با تزریق مایع از دیواره پایینی آن بررسی شده است. شرایط عدم لغزش در دیواره میکروکانال در نظر گرفته شده است و شرط مرزی برای دیواره‌های بالایی و پایین مجرای سرریز به عنوان عایق و دمای ثابت در نظر گرفته می‌شود. نتایج نشان داده شده است که موقعیت لایه متخلخل تاثیر قابل توجهی بر انتقال گرما دارد. درصد تغییر در عدد ناسلت برای مواردی مشاهده می‌شود که در آن لایه متخلخل در دیواره فوقانی و نزدیک دیواره فوقانی و در شکل یک دنده و در بخش بخش تقسیم شده شده بر $L/3$ و $L/5$ ترتیب، 2.25% ، 5.46% ، 70.5% و 86.27% در مقایسه با حالت بدون لایه متخلخل بوده است.
